

L3. Radial Functions

- The radial functions $j_j^{(l'm)}(x)$ and $\pm 2j_j^{(l'm)}(x)$ determine the free streaming of multipoles according to Eqs. (2.15) and (2.38). For the line-of-sight integrals (2.22) and (2.45) we need the $j_j^{(l'm)}$ only up to $l'=2$ (and $m=0, \dots, \pm l'$), and $\pm 2j_j^{(2m)} = \varepsilon_j^m \pm i\beta_j^m$ for $m=0, \pm 1, \pm 2$.
- The radial functions $j_j^{(l'm)}$ are given by the Clebsch-Gordan series as (2.14)

$$j_j^{(l'm)} \equiv \sum_l (-i)^{l+l'-j} \left(\frac{2l+1}{2j+1}\right) \langle l_0 l' m | j_m \rangle \langle l_0 l' 0 | j_0 \rangle j_L \quad (1)$$

as linear combinations of spherical Bessel functions.

- We shall need some properties of the spherical Bessel functions $j_L(x)$:

Recursion formulae:

(' \equiv derivative)

$$(2l+1) j_L' = l \cdot j_{L-1} - (l+1) \cdot j_{L+1} \quad (2)$$

$$(2l+1) \frac{j_L(x)}{x} = j_{L-1}(x) + j_{L+1}(x) \quad (3)$$

Value at zero:

$$\underline{j_L(0) = \delta_{L0}} \quad (4)$$

- For $(l'm) = (00)$, we simply have $j_j^{(00)} = j_j$ since $\langle l_0 0 0 | j_0 \rangle = \delta_{L0}$.

In general, the $\langle l_0 l' m | j_m \rangle$ can be nonzero only for $l = |j-l'|, \dots, j+l'$.

Moreover, since $\langle l_0 l' 0 | j_0 \rangle = 0$ for $l+l'-j$ odd, (1) turns out to be real, and

the $l'=1$ case has only 2 terms: $l=j-1, j+1$ and the $l'=2$ case has only

3 terms: $l=j-2, 0, j+2$ in the series (1).

- Using the values for $\langle l_0 l' m | j_m \rangle$ given by VMK Tables 8.2 and 8.4 and from the recursion formulae (2) and (3) we get the following result

for $j_j^{(l'm)}$ (next page).

- The radial functions $j_L^{(l'm)}(x)$

$$\begin{aligned}
 j_L^{(00)} &= j_L \\
 j_L^{(10)} &= \frac{l}{2L+1} j_{L-1} - \frac{L+1}{2L+1} j_{L+1} \\
 j_L^{(20)} &= \frac{3}{2} \frac{l(l-1)}{(2L+1)(2L-1)} j_{L-2} - \frac{l(l+1)}{(2L+3)(2L-1)} j_L + \frac{3}{2} \frac{(L+2)(L+1)}{(2L+3)(2L+1)} j_{L+2} \\
 j_L^{(11)} &= \frac{1}{2L+1} \sqrt{\frac{l(l+1)}{2}} (j_{L-1} + j_{L+1}) \\
 j_L^{(21)} &= \sqrt{\frac{3}{2} l(l+1)} \left[\frac{l-1}{(2L+1)(2L-1)} j_{L-2} - \frac{l}{(2L-1)(2L+3)} j_L - \frac{l+2}{(2L+1)(2L+3)} j_{L+2} \right] \\
 j_L^{(22)} &= \sqrt{\frac{3}{8} (L-1) l (L+1) (L+2)} \left[\frac{1}{(2L+1)(2L-1)} j_{L-2} + \frac{2}{(2L-1)(2L+3)} j_L + \frac{1}{(2L+1)(2L+3)} j_{L+2} \right]
 \end{aligned} \tag{5}$$

$$\underline{j_L^{(l',m)}} = j_L^{(l'm)} \tag{6}$$

- Using the recursion formulae (2) & (3) we can put these into a form where only the same j_L appears in each term:

$$\begin{aligned}
 j_L^{(00)} &= j_L & j_L^{(11)}(x) &= \sqrt{\frac{l(l+1)}{2}} \frac{j_L(x)}{x} \\
 j_L^{(10)} &= j_L' & j_L^{(21)}(x) &= \sqrt{\frac{3}{2} l(l+1)} \left(\frac{j_L(x)}{x} \right)' \\
 j_L^{(20)} &= \frac{3}{2} j_L'' + \frac{1}{2} j_L & j_L^{(22)}(x) &= \sqrt{\frac{3}{8} (L-1) l (L+1) (L+2)} \frac{j_L(x)}{x^2}
 \end{aligned} \tag{7}$$

- To show by substitution that (2.22) satisfies (2.1a) we need the recursion relation

$$(2L+1) j_L^{(l'm)}' = \sqrt{l^2 - m^2} j_{L-1}^{(l'm)} - \sqrt{(L+1)^2 - m^2} j_{L+1}^{(l'm)} \tag{8}$$

(I have verified this only for (00), (10), (20), (11)) and the values at zero

$$\underline{j_L^{(l'm)}(0)} = \frac{1}{2L+1} \delta_{ll'} \tag{9}$$

- Note also that

$$\underline{j_L^{(00)}} = j_L^{(10)}$$

$$\underline{j_L^{(10)}} = \frac{2}{3} j_L^{(20)} - \frac{1}{3} j_L^{(00)} \quad \underline{j_L^{(11)'}} = \frac{1}{\sqrt{3}} j_L^{(21)} \tag{10}$$

- The polarization radial functions $\pm_2 j_j^{(l,m)}$ are given by (36) as

$$\pm_2 j_j^{(2m)} \equiv \sum_l (-i)^{l+2-j} \left(\frac{2l+1}{2j+1} \right) \langle l 0 2m | j_m \rangle \langle l 0 j, \mp 2 | j, \mp 2 \rangle j_l \quad (11)$$

- The complex phase of the terms comes from $(-i)^{l+2-j}$ \Rightarrow the $l=j-1, j+1$ terms are imaginary and the others are real. Examination of VMK Table 8.4 reveals that

$$\langle j^{\pm 1}, 0; j, +2 | j, +2 \rangle = - \langle j^{\pm 1}, 0; j, -2 | j, -2 \rangle \Rightarrow \underline{-_2 j_j^{(2m)}} = \underline{+_2 j_j^{(2m)*}} \quad (12)$$

\therefore Thus we can write $\underline{\pm_2 j_j^{(2m)}} = \underline{\epsilon_j^m \pm i\beta_j^m}$ where ϵ_j^m, β_j^m are real. \square (13)

- From VMK Table 8.4 we also see that $\langle l 0 j, -m | j, -m \rangle = (-1)^{l+j} \langle l 0 j, m | j, m \rangle$, meaning that the imaginary terms (i.e. the β_j^m) get the opposite sign for $-m$.

$$\Rightarrow \underline{2 j_j^{(2,-m)}} = \underline{2 j_j^{(2m)*}} \Rightarrow \boxed{\begin{aligned} \epsilon_j^{-m} &= \epsilon_j^m \\ \beta_j^{-m} &= -\beta_j^m \end{aligned}} \quad (14)$$

Combining (12) & (14), we have $\underline{2 j_j^{(2,-m)}} = \underline{2 j_j^{(2m)*}} = \underline{-_2 j_j^{(2m)}} = \underline{-_2 j_j^{(2,-m)*}}$ (15)

We also see from (14) that $\beta_j^0 = 0$. (16)

- Comparing (11) to (1), we note that $\underline{\pm_2 j_j^{(20)}} = \underline{\epsilon_j^0} = \underline{j_j^{(2,\mp 2)}} = \underline{j_j^{(22)}}$ (17)

- Using VMK Table 3.4 we get from (11) & (13) that

$$\begin{aligned}
 \mathcal{E}_l^0 &= j_l^{(22)} \\
 \mathcal{E}_l^1 &= \frac{1}{2} \sqrt{(l-1)(l+2)} \left[\frac{l+1}{(2l+1)(2l-1)} j_{l-2} + \frac{3}{(2l-1)(2l+3)} j_l - \frac{l}{(2l+1)(2l+3)} j_{l+2} \right] \\
 \mathcal{E}_l^2 &= \frac{1}{4} \left[\frac{(l+1)(l+2)}{(2l-1)(2l+1)} j_{l-2} - 6 \frac{(l-1)(l+2)}{(2l-1)(2l+3)} j_l + \frac{(l-1)l}{(2l+1)(2l+3)} j_{l+2} \right] \\
 \beta_l^0 &= 0 \\
 \beta_l^1 &= \frac{\sqrt{(l-1)(l+2)}}{2(2l+1)} [j_{l-1} + j_{l+1}] \\
 \beta_l^2 &= \frac{1}{2(2l+1)} [(l+2)j_{l-1} - (l-1)j_{l+1}]
 \end{aligned} \tag{18}$$

- Using the recursion relations (2) & (3) we can put these into the form

$$\begin{aligned}
 \mathcal{E}_l^0(x) &= \sqrt{\frac{3}{8}(l-1)l(l+1)(l+2)} \frac{j_l(x)}{x^2} & \beta_l^0(x) &= 0 \\
 \mathcal{E}_l^1(x) &= \frac{1}{2} \sqrt{(l-1)(l+2)} \left[\frac{j_l(x)}{x^2} + \frac{j_l'(x)}{x} \right] & \beta_l^1(x) &= \frac{1}{2} \sqrt{(l-1)(l+2)} \frac{j_l(x)}{x} \\
 \mathcal{E}_l^2(x) &= \frac{1}{4} \left[-j_l(x) + j_l''(x) + 2 \frac{j_l(x)}{x^2} + 4 \frac{j_l'(x)}{x} \right] & \beta_l^2(x) &= \frac{1}{2} \left[j_l'(x) + 2 \frac{j_l(x)}{x} \right]
 \end{aligned} \tag{19}$$

$$C_{\alpha\beta\gamma}^{\chi} \equiv \langle \alpha\alpha b\beta | c\gamma \rangle$$

Table 8.2
 $C_{\alpha\beta\gamma}^{CT}$

c	$\beta = 1$	$\beta = 0$	$\beta = -1$
$a+1$	$\left[\frac{(c+\gamma-1)(c+\gamma)}{(2c-1)2c} \right]^{1/2}$	$\left[\frac{-(c+\gamma)(c-\gamma)}{(2c-1)c} \right]^{1/2}$	$\left[\frac{(c-\gamma-1)(c-\gamma)}{(2c-1)2c} \right]^{1/2}$
a	$-\left[\frac{(c+\gamma)(c-\gamma+1)}{2c(c+1)} \right]^{1/2}$	$\frac{1}{\left[\frac{c(c+1)}{2c(c+1)} \right]^{1/2}}$	$\left[\frac{(c+\gamma+1)(c-\gamma)}{2c(c+1)} \right]^{1/2}$
$a-1$	$\left[\frac{(c-\gamma+1)(c-\gamma+2)}{(2c+2)(2c+3)} \right]^{1/2}$	$-\left[\frac{(c+\gamma+1)(c-\gamma+1)}{(c+1)(2c+3)} \right]^{1/2}$	$\left[\frac{(c+\gamma+2)(c-\gamma+1)}{(2c+2)(2c+3)} \right]^{1/2}$

Table 8.4
 $C_{\alpha\beta\gamma}^{CT}$

c	$\beta = 2$	$\beta = 1$
$a+2$	$\left[\frac{(c+\gamma-3)(c+\gamma-2)(c+\gamma-1)(c+\gamma)}{(2c-3)(2c-2)(2c-1)2c} \right]^{1/2}$	$\left[\frac{(c+\gamma-2)(c+\gamma-1)(c+\gamma)(c-\gamma)}{(2c-3)(c-1)(2c-1)c} \right]^{1/2}$
$a+1$	$-\left[\frac{(c+\gamma-2)(c+\gamma-1)(c+\gamma)(c-\gamma+1)}{(2c-2)(2c-1)c(c+1)} \right]^{1/2}$	$-(c-2\gamma+1)\left[\frac{(c+\gamma-1)(c-\gamma)}{(2c-2)(2c-1)c(c+1)} \right]^{1/2}$
a	$\left[\frac{3(c+\gamma-1)(c+\gamma)(c-\gamma+1)(c-\gamma+2)}{(2c-1)c(c+1)(2c-3)} \right]^{1/2}$	$(1-2\gamma)\left[\frac{3(c+\gamma)(c-\gamma+1)}{2(2c-1)c(c+1)(2c+3)} \right]^{1/2}$
$a-1$	$\left[\frac{(c+\gamma)(c-\gamma+1)(c-\gamma+2)(c-\gamma+3)}{c(c+1)(2c+3)(2c+4)} \right]^{1/2}$	$(c+2\gamma)\left[\frac{(c-\gamma+1)(c-\gamma+2)(c-\gamma+3)}{c(c+1)(2c+3)(2c+4)} \right]^{1/2}$
$a-2$	$\left[\frac{(c-\gamma+1)(c-\gamma+2)(c-\gamma+3)(c-\gamma+4)}{(2c+2)(2c+3)(2c+5)} \right]^{1/2}$	$-(c+1)(2c+3)(c+2)(2c+5)$

Table 8.4. (Cont.)

c	$\beta = 0$	$\beta = -1$	$\beta = -2$
$a+2$	$\left[\frac{3(c+\gamma-1)(c+\gamma)(c-\gamma-2)(c-\gamma-1)(c-\gamma)}{(2c-3)(2c-2)(2c-1)c} \right]^{1/2}$	$\left[\frac{(c+\gamma)(c-\gamma-2)(c-\gamma-1)(c-\gamma)}{(2c-3)(c-1)(2c-1)c} \right]^{1/2}$	$\left[\frac{(c-\gamma-3)(c-\gamma-2)(c-\gamma-1)(c-\gamma)}{(2c-3)(2c-2)(2c-1)c} \right]^{1/2}$
$a+1$	$\gamma\left[\frac{3(c+\gamma)(c-\gamma)}{(c-1)(2c-1)c(c+1)} \right]^{1/2}$	$(c+2\gamma+1)\left[\frac{(c-\gamma-1)(c-\gamma)}{(2c-2)(2c-1)c(c+1)} \right]^{1/2}$	$\left[\frac{(c+\gamma+1)(c-\gamma-2)(c-\gamma-1)(c-\gamma)}{(2c-2)(2c-1)c(c+1)} \right]^{1/2}$
a	$\frac{[(2c-1)c(c+1)(2c+3)]^{1/2}}{3\gamma^2 - c(c+1)}$	$(2\gamma+1)\left[\frac{3(c+\gamma+1)(c-\gamma)}{2(2c-1)c(c+1)(2c+3)} \right]^{1/2}$	$\left[\frac{3(c+\gamma+1)(c-\gamma-1)(c-\gamma)}{2(2c-1)c(c+1)(2c+3)} \right]^{1/2}$
$a-1$	$-\gamma\left[\frac{3(c+\gamma+1)(c-\gamma+1)}{c(c+1)(2c+3)(c+2)} \right]^{1/2}$	$-(c-2\gamma)\left[\frac{(c+\gamma+1)(c-\gamma+2)}{c(c+1)(2c+3)(2c+4)} \right]^{1/2}$	$\left[\frac{(c+\gamma+1)(c-\gamma+2)(c-\gamma+3)}{c(c+1)(2c+3)(2c+4)} \right]^{1/2}$
$a-2$	$\left[\frac{3(c+\gamma+1)(c+\gamma+2)(c-\gamma+1)(c-\gamma+2)}{(c+1)(2c+3)(2c+4)(2c+5)} \right]^{1/2}$	$-\left[\frac{(c+\gamma+1)(c+\gamma+2)(c+\gamma+3)(c+\gamma+4)}{(c+1)(2c+3)(2c+5)(2c+6)} \right]^{1/2}$	$\left[\frac{(c+\gamma+1)(c+\gamma+2)(c+\gamma+3)(c+\gamma+4)}{(2c+2)(2c+3)(2c+5)(2c+6)} \right]^{1/2}$

$$j_\ell^{(10)}(x) = j_\ell'(x),$$

$$[j_\ell''(x) + j_\ell(x)],$$

$$\frac{\ell(\ell+1)}{2} \frac{j_\ell(x)}{x},$$

$$\frac{\ell(\ell+1)}{2} \left(\frac{j_\ell(x)}{x} \right)',$$

$$\frac{3(\ell+2)!}{3(\ell-2)!} \frac{j_\ell(x)}{x^2} \quad (15)$$

ivatives with respect to the ar-
 $x=kr$. These modes are shown

functions with $m>0$ (see Fig.

$$\frac{1}{4\pi(2\ell+1)} [\epsilon_\ell^{(m)}(kr)$$

$$]_{\pm 2} Y_\ell^m(\hat{n}), \quad (16)$$

$$\frac{(\ell+2)!}{(\ell-2)!} \frac{j_\ell(x)}{x^2},$$

$$\frac{1}{\ell+2} \left[\frac{j_\ell(x)}{x^2} + \frac{j_\ell'(x)}{x} \right],$$

$$''(x) + 2 \frac{j_\ell(x)}{x^2} + 4 \frac{j_\ell'(x)}{x}], \quad (17)$$

$=\ell, \ell \pm 2$ coupling and

$$x=0,$$

$$\frac{-1}{(\ell+2)} \frac{j_\ell(x)}{x},$$

$$'(x) + 2 \frac{j_\ell(x)}{x}], \quad (18)$$

$=\ell \pm 1$ coupling. The corre-
 \rightarrow involves a reversal in sign:

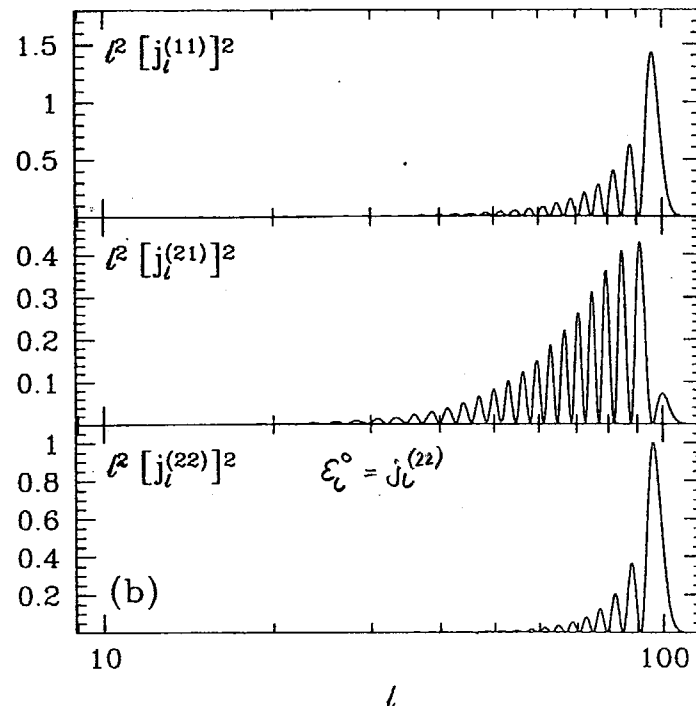
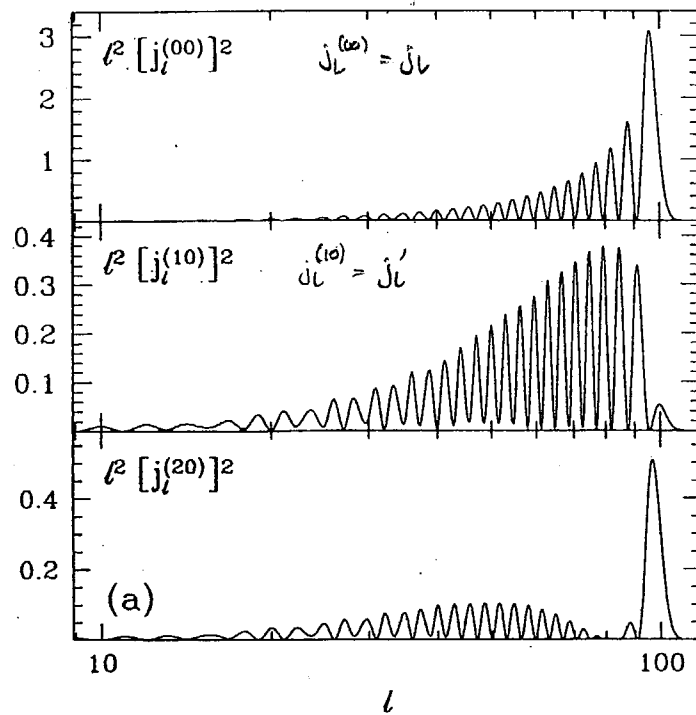


FIG. 3. Radial spin-0 (temperature) modes. The angular power in a plane wave (left panel, top) is modified due to the intrinsic angular structure of the source as discussed in the text. The left panel corresponds to the power in scalar ($m=0$) monopole G_0^0 , dipole G_1^0 , and quadrupole G_2^0 sources (top to bottom); the right panel to that in vector ($m=1$) dipole $G_1^{\pm 1}$ and quadrupole $G_2^{\pm 1}$ sources and a tensor ($m=2$) quadrupole $G_2^{\pm 2}$ source (top to bottom). Note the differences in how sharply peaked the power is at $\ell \approx kr$ and how fast power falls as $\ell \ll kr$. The argument of the radial functions $kr=100$ here.

to a range of angular scales from $\ell \approx kr$ at $\theta = \pi/2$ to larger angles $\ell \approx kr$ as $\theta \approx 0^\circ$ ($\ell \approx kr$ where $\hat{k} \cdot \hat{n} = \cos \theta$ (see Fig. 1))

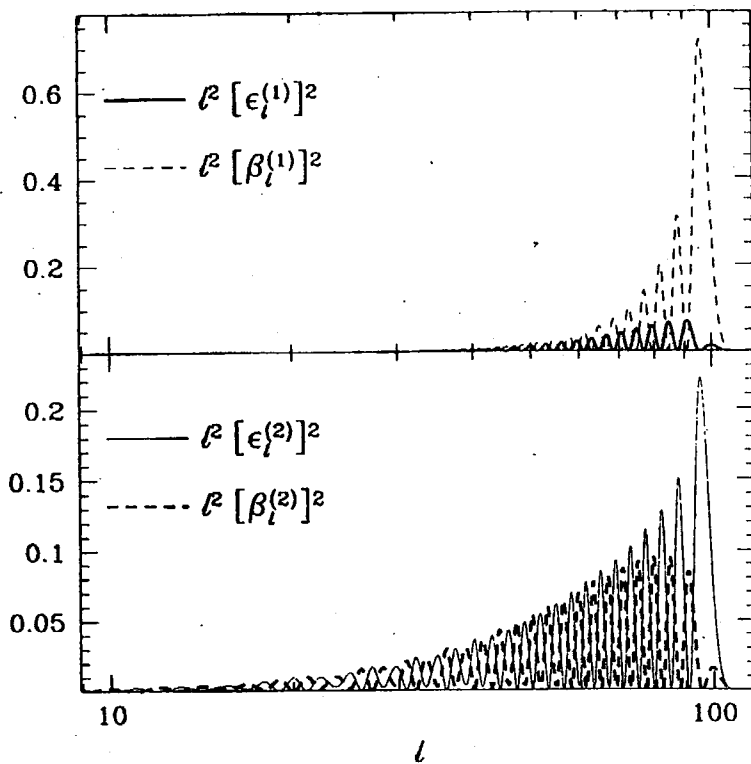


FIG. 4. Radial spin-2 (polarization) modes. Displayed is the angular power in a plane-wave spin-2 source. The top panel shows that vector ($m=1$, upper panel) sources are dominated by B -parity contributions, whereas tensor ($m=2$, lower panel) sources have comparable but less power in the B parity. Note that the power is strongly peaked at $\ell=kr$ for the B -parity vectors and E -parity tensors. The argument of the radial functions $kr=100$ here.

Thus factors of $\sin\theta$ in the intrinsic angular dependence suppress power at $\ell \ll kr$ (“aliasing suppression”), whereas factors of $\cos\theta$ suppress power at $\ell \approx kr$ (“projection suppression”). Let us consider first a $m=0$ dipole contribution $Y_1^0 \propto \cos\theta$ (see Fig. 2). The $\cos\theta$ dependence suppresses power in $j_{\ell}^{(10)}$ at the peak in the plane-wave spectrum $\ell \approx kr$ [compare Fig. 3(a) top and middle panels]. The remaining power is broadly distributed for $\ell \leq kr$. The same reasoning applies for Y_2^0 quadrupole sources which have an intrinsic angular dependence of $3\cos^2\theta - 1$. Now the minimum falls at $\theta = \cos^{-1}(1/\sqrt{3})$ causing the double peaked form of the power in $j_{\ell}^{(20)}$ shown in Fig. 3(a) (bottom panel). This series can be continued to higher G_{ℓ}^0 and such techniques have been used in the free streaming limit for temperature anisotropies [11].

Similarly, the structures of $j_{\ell}^{(11)}$, $j_{\ell}^{(21)}$, and $j_{\ell}^{(22)}$ are apparent from the intrinsic angular dependences of the G_{ℓ}^1 ,

Secondly, even wavelength sources angle anisotropies a

This scaling puts a can rise with / the bound on the amou that *decreases* with

The same argu the added complica tions ϵ_{ℓ} and β_{ℓ} . introduces a β cont $m=\pm 1$, the β cor contributions; whe slightly larger than reach the asymptoti

$$\frac{\Sigma_{\ell}[\ell]}{\Sigma_{\ell}[\ell]}$$

for fixed $kr \gg 1$. Tl the parity of the n angular momentum does mix states of c does not have defin in the intrinsic ang

$${}_2G_2^m \mathbf{M}_+ + {}_{-2}G$$

Thus the addition generates ‘‘magnet an intrinsically ‘‘e parity of amplitude functions has sign calculation in Sec. tion is absent for s